An Experimental Study of the Cylindrical Langmuir Probe Response in the Transition Regime

R. H. KIRCHHOFF,* E. W. PETERSON,† AND L. TALBOT‡
University of California, Berkeley, Calif.

A study of the response of cylindrical Langmuir probes in the transition regime has been made. Experiments were performed in a highly expanded low-density flowing argon plasma using both single and double probes. Results are obtained in the near free-molecule regime over a wide range of ratios of Debye length to probe radius, probe length to probe radius, and probe radius to relevant mean free path. The effect of collisions on the ion-saturation current, the retarding field electron current, the floating potential, and the inferred electron temperature have been investigated experimentally. An existing approximate analysis describing the collisional single probe ion-saturation current and the retarding field electron current has been extended to describe the collisional double probe characteristic and magnitude of the single probe floating potential.

Nomenclature

A = probe area
D = throat diameter
E_1, Ei = exponential integrals
e = one electronic charge (absolute value)
f = tabulated in Table 1 [see Eq. (1)]
G = tabulated in Table 1 [see Eqs. (2) and (6)]
h = current in double-probe circuit, normalized with respect to probe 1
J = probe current
J_r = $n(kT/2\pi m)^{1/2}Aze$ random thermal current
j = J/J_r normalized probe current
K = λ/r Knudsen number
k = Boltzmann constant
l = probe length
M = Mach number
m = particle mass
n = number density
R = Reynolds number
r = probe radius
r_s = sheath radius in the continuum limit
T = temperature
U = freestream velocity
V = applied probe-to-probe or probe-to-reference-voltage
x = axial distance
x_0 = defined by Eq. (3), $x_0 = r_s/r$
Y = defined by Eq. (14)
Z = defined by Eq. (14)
z = number of electronic charges on particle
α = defined by Eq. (1) and Fig. 1
β = defined by Eq. (4)
γ = defined by Eq. (2)
δ = defined by Eq. (6)
θ = kT/e temperature, ev
λ = length (with subscripts as indicated below for mean-free-path or d for Debye length)
ξ = r/λ_d
σ = defined by Eq. (14)
τ = T_e/T_i
ϕ = potential measured with respect to plasma potential
χ = $-e\phi/kT_e$ normalized potential
ψ = eV/kT_e normalized potential

Subscripts

1,2 = numerical designation for double-probe electrodes
∞ = collisionless limit
e = electron
f = the probe open circuit potential
i = ion
n = neutral particle
0 = collisional limit
p = probe surface
ce = charge exchange

Superscript

* = ion current referred to electron temperature $j_i^* = j_i/(\tau)^{1/2}$

Presented as Paper 70-85 at the AIAA 8th Aerospace Sciences Meeting, New York, January 19–21, 1970; submitted March 9, 1970; revision received November 2, 1970. This research was supported by the Air Force Office of Scientific Research under AFOSR Grant 538-67.

* Graduate Student; presently Assistant Professor, University of Massachusetts. Member AIAA.
† Graduate Student; presently Assistant Professor, University of Minnesota. Member AIAA.
‡ Professor of Aeronautical Sciences. Member AIAA.

1.0 Introduction

THE Langmuir probe is widely used as a diagnostic tool to measure local properties of plasmas. Such quantities as the charged particle density, electron temperature, and plasma potential may under appropriate circumstances be determined from the characteristic that is produced when the current drawn between the probe and a reference electrode is recorded as a function of applied voltage. This probe response is best understood in the collisionless regime and under certain restrictions the response is also known in the continuum regime. However, operation under these conditions is often not possible and it is therefore useful to investigate the response in the transition regime.

Several attempts have been made[1–7] to understand the response of Langmuir probes in the transition regime. To date, experimental results on the transition regime have been restricted to investigating effects on the ion-saturation current for values of $r/\lambda_d < 10$ as reported by Kaegi and Chin[8] and Dunn and Lordi.[10] The most complete theory appears to be that of Chou, Talbot and Willis[6]; however, the numerical computations presented in Ref. 6 are not extensive enough for the purposes of the experimentalist. Recently Talbot and Chou[9] completed an approximate analysis which permits the calculation of the effect of collisions on the ion-saturation current and the electron current in the electron-retarding field

Table 1 Functions for the evaluation of the probe current

	$\tau = 1$	$\tau = 2$	$\tau = 5$	$\tau = 10$	$\tau = \infty$
$f(\tau)$	1.38	1.18	1.04	0.99	0.94
$G_i(\tau)$	1.07	0.89	0.70	0.58	...
$G_e(\tau)$	2.52	2.20	1.84	1.58	...

region for both cylindrical and spherical probes. The analysis was found to compare favorably with the ion-saturation current measurements of Kaegi and Chin. However, at that time electron current data were not available with which to make meaningful comparisons in the electron-retarding region.

The purpose of the present work is to determine experimentally the single-probe and double-probe characteristics in the near free-molecule regime for a wide range of ratios of Debye length to probe radius, probe length to radius, and probe radius to relevant mean-free-path in the plasma. Single-probe data are obtained in the ion-saturation and electron-retarding regions, and the collisional influences on measurements of charged particle number density and electron temperature are exhibited. Direct measurements are made of the single-probe floating potential, using the plasma potential as reference, and the resulting collisional effects are shown. The measurements of electron temperature and charged particle number density from a double-probe characteristic taken in the near free-molecule regime are also investigated.

The Talbot-Chou[9] approximate analysis, describing the effect of collisions on the single-probe ion-saturation and electron currents in the electron-retarding region, is extended to describe the effect of collisions on the double-probe characteristic and on the single-probe floating potential. An implicit expression for the double-probe electron temperature is also derived. Qualitative comparisons are made between theory and experiment, and the use of the Langmuir probe as a plasma diagnostic tool in the near free-molecule regime is discussed.

2.0 Theory

2.1 Transition Regime

An approximate analysis was presented by Talbot and Chou[9] which permits the calculation of the effect of collisions on the ion-saturation current and the electron current in the electron-retarding region for both cylindrical and spherical electrostatic probes. Since this analysis provides the foundation for the theoretical formulation of the double-probe characteristic, and the computation of the single-probe floating potential, and because these results are used to provide comparisons with the experiment, a brief review of the Talbot-Chou analysis is given here. Their approximate analysis is based on an earlier theory of Chou, Talbot and Willis[6] for the response of a spherical, perfectly absorbing, Langmuir probe operating in the transition regime in a weakly ionized gas. This theory makes use of a moment approximation to the Boltzmann equation with a Krook-type collision integral where the dominant collisions are assumed to be those between charged and neutral particles. No restrictions are placed on the Knudsen number or the ratio of Debye length to probe radius. In the analysis certain integrals of the potential over the region between the undisturbed plasma and the probe arise. These integrals were evaluated numerically for several sets of the relevant parameters in order to establish the trends of the results; however, the numerical work was not extensive enough for the purposes of the experimentalist. The intent of the Talbot-Chou analysis was to provide simple approximations for these integrals covering the entire range of interest. In essence they found representations for these integrals in the collisionless and continuum limits, and an interpolation formula was then used to obtain values for these integrals in the transition region between these limits. The approach was followed for both spherical and cylindrical probes, although only the latter results will be used in this report.

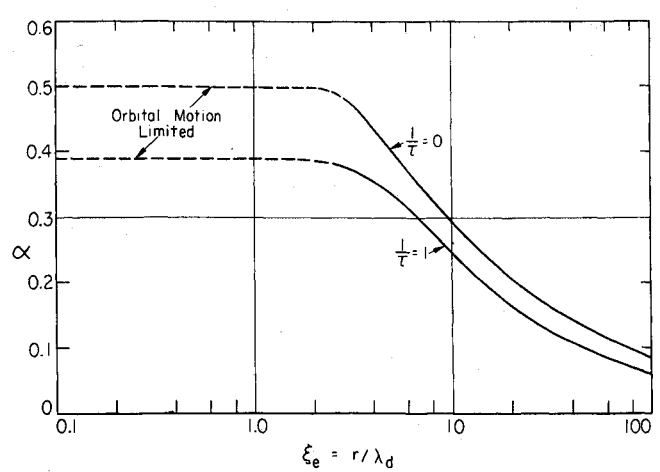

Fig. 1 Correlation exponent in Eq. (1) for collisionless ion current to a cylindrical probe.

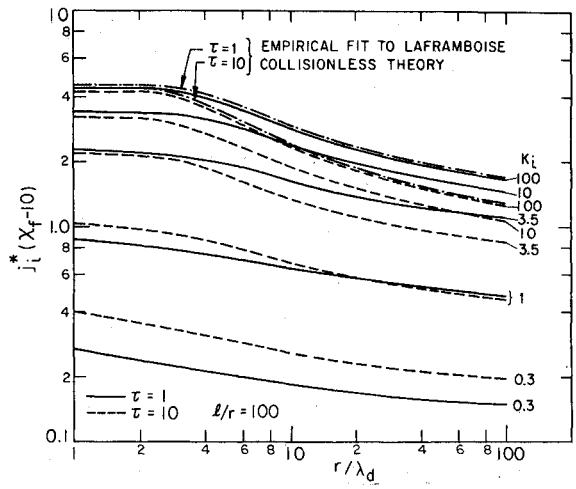

Fig. 2 Transitional ion current at ten dimensionless volts below the probe floating potential, vs r/λ_d and K_i.

The normalized ion-saturation current to a cylindrical probe in the transition regime is[9]

$$j_i^* = j_{i,\infty}^* \gamma = \frac{J_i}{z2\pi rl(kT_e/2\pi m_i)^{1/2} n_i e} = \frac{J_i}{J_r} \qquad (1)$$

$$zn_i = n_e$$

where $j_{i,\infty}^* = f(\tau)(\chi_p/\chi_c)^\alpha$ is an approximation to the collisionless ion-saturation current calculations of Laframboise[11] and γ is defined by

$$\gamma^{-1} = 1 + \tau^{1/2}K_i^{-1}(G_i(\tau)(j_{i,\infty}^*)^{1/2} + \alpha j_{i,\infty}^*[E_1(\tau \ln 2) - E_1(\tau\chi_p)] + (1 + K_i)^{-1}\{[1/(1 + \tau)]j_{i,\infty}^* \ln(l/rx_0) - G_i(\tau)(j_{i,\infty}^*)^{1/2} - \alpha j_{i,\infty}^*[E_1(\tau \ln 2) - E_1(\tau\chi_p)]\}) \qquad (2)$$

The term E_1 is the exponential integral

$$E_1(\tau) = \int_\tau^\infty \exp(-t)\left(\frac{dt}{t}\right)$$

tabulated by Abramowitz and Stegun,[12] $G_i(\tau)$ and $f(\tau)$ are given in Table 1, α is given in Fig. 1, $\chi_c = \ln 2$ for cylindrical probes, and x_0 may be estimated from

$$\chi_p\beta^{-1/2} = x_0 \ln\{(x_0^2 - 1)^{1/2} + x_0\} - (x_0^2 - 1)^{1/2} \qquad (3)$$

$$\beta = j_{i,0}\xi_e^2/K_i\tau \qquad (4)$$

$$\xi_e = r/(\epsilon_0 kT_e/e^2 n_e)^{1/2} = r/\lambda_d$$

where the normalized continuum-limit current was taken to be given by[13] $j_{i,0} = K_i(1 + \tau)/\ln(l/rx_0)$. A plot of j_i^* vs K_i and r/λ_d at ten dimensionless volts below floating potential is given in Fig. 2. Collisions have the effect of reducing the

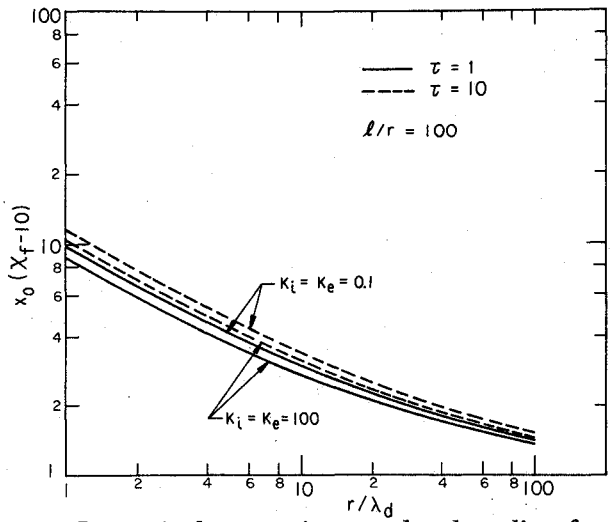

Fig. 3 Dimensionless continuum sheath radius for a cylindrical probe.

ion current to the probe and thus reduce the apparent number density inferred from collisionless theory. Figure 3 is a plot of the dimensionless ion sheath radius from Eq. (3). Although $\chi_p\beta^{-1/2}$ is independent of K_i, the value of the floating potential χ_f does depend on K_i, and thus when x_0 is plotted for the particular probe potential $\chi_p = \chi_f - 10$, a small Knudsen number dependence results. For large negative probe potentials this Knudsen number dependence becomes negligible.

The electron current in the electron-retarding field is given approximately by[9]

$$j_e = \delta \exp(-\chi_p) \tag{5}$$

where δ is defined by

$$\delta^{-1} = 1 + K_e^{-1}\exp(-\chi_p)\{G_e(\tau)(j_{i,\infty}^*)^{-1/2} + \alpha[Ei(\chi_p) - Ei(\ln 2)] + (1 + K_e)^{-1}\{\chi_p \ln(lx_0/r) - G_e(\tau)(j_{i,\infty}^*)^{-1/2} - \alpha[Ei(\chi_p) - Ei(\ln 2)]\}\} \tag{6}$$

The term Ei is the exponential integral

$$Ei(y) = \int_{-\infty}^{y} \exp(t)\,\frac{dt}{t}$$

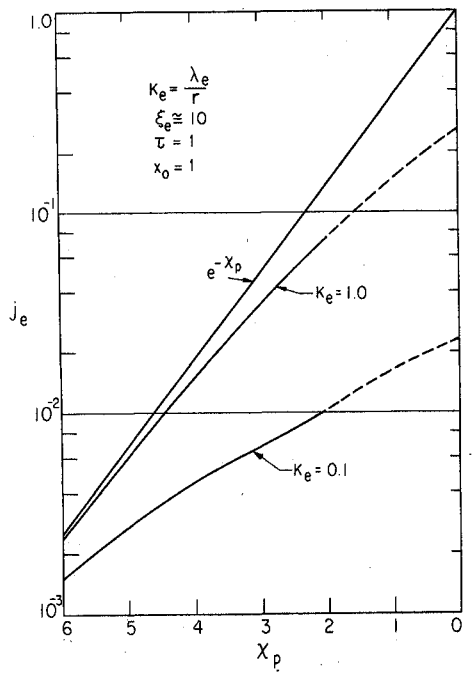

Fig. 4 Theoretical prediction of transitional effects on probe electron current in the retarding-field regime.

tabulated in Ref. 12, $G_e(\tau)$ is given in Table 1, and x_0 may be estimated as described above. Representative curves of the logarithm of the normalized electron current (j_e) are given in Fig. 4 as a function of the nondimensional potential χ_p. The curves shown were extrapolated to the $\chi_p = 0$ limit,

$$j_e(\chi_p = 0) = (1 + K_e^{-1}\{1 + (1 + K_e)^{-1}[\ln(lx_0/r) - 1]\})^{-1} \tag{7}$$

as given in Ref. 9. Note that the electron-current characteristics depart progressively more from a straight line as the Knudsen number decreases, and as K_e becomes quite small a pronounced inflection point appears in the curve. In the collisionless limit, the electron temperature may be computed from the slope of the logarithm of the electron current in the electron-retarding field region. However, it is apparent that if the electron current has the behavior predicted in Fig. 4, it would be extremely difficult to compute the electron temperature directly from the characteristics obtained in the transition regime.

The results of the Talbot-Chou analysis, summarized by Eqs. (1–6), may be used to compute the potential at which the probe will collect equal amounts of ion and electron current. The normalized "floating potential," χ_f, measured with respect to the plasma potential at which $j_i^* = j_e$ is found from Eqs. (1) and (5) to be

$$\chi_f = \tfrac{1}{2}\ln(m_i/m_e) - \ln\{f(\tau)(\chi_f/\chi_c)^{\alpha}\} - \ln\gamma + \ln\delta \tag{8}$$

Representative values of the probe floating potential in the transition regime are shown in Fig. 5. The most important result to be noted is that the analysis predicts an increase in the magnitude of χ_f as the Knudsen number decreases.

The current-voltage characteristic describing the double-probe response in the transition regime may also be determined from Eqs. (1) and (5). Assume probes 1 and 2, having equal radii but with areas A_1 and A_2, respectively, are located in a plasma having constant properties within the probe spacing. Then the current h^* in the double-probe circuit, normalized with respect to probe 1, must be

$$h^* = (A_2/A_1)\{j_{i2}^* - (m_i/m_e)^{1/2}j_{e2}\} = (m_i/m_e)^{1/2}j_{e1} - j_{i1}^* \tag{9}$$

in order to satisfy continuity requirements. If the normalized voltage applied between the two probes is defined by

$$\psi = eV/kT_e = \chi_{p1} - \chi_{p2} \tag{10}$$

then the double-probe characteristic (h^* vs ψ)

$$h^* = A_2/A_1[j_{i2}^* - j_{i1}^*(\delta_2/\delta_1)\exp\psi][1 + (A_2/A_1)(\delta_2/\delta_1)\exp\psi]^{-1} \tag{11}$$

is found from Eqs. (9) and (10). In the collisionless limit, the electron temperature is usually calculated from the slope of

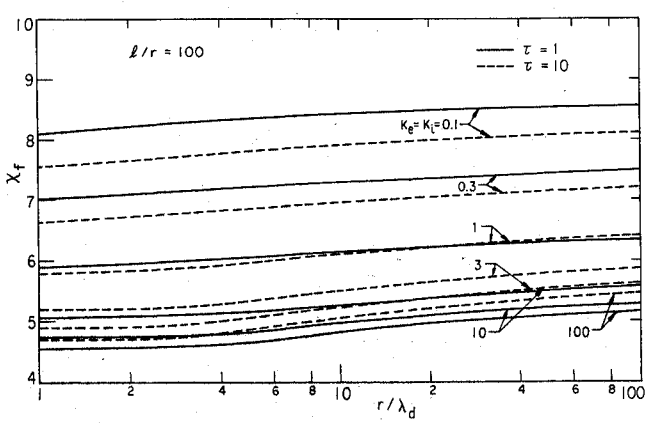

Fig. 5 Prediction of probe floating potential variation with Knudsen number.

this curve and the magnitudes of the ion currents, all evaluated at $\psi = 0$. The analogous relation for the electron temperature measurement in the near free molecule regime may be found using Eqs. (1, 10, and 11). From Eq. (11) the slope of the double-probe characteristic is

$$\frac{\partial h^*}{\partial V} = \frac{A_2}{A_1}\left(\frac{\partial j_{i_2}^*}{\partial V} - \frac{\partial j_{i_1}^*}{\partial V}\frac{\delta_2}{\delta_1}\exp\psi - \frac{j_{i_1}^*}{\delta_1}\frac{\partial \delta_2}{\partial V}\exp\psi + \frac{j_{i_1}^*\delta_2}{\delta_1^2}\frac{\partial \delta_1}{\partial V}\exp\psi - \theta_e^{-1}\frac{j_{i_1}^*\delta_2}{\delta_1}\exp\psi\right)\left(1 + \frac{A_2}{A_1}\frac{\delta_2}{\delta_1}\exp\psi\right)^{-1} - h^*\left(1 + \frac{A_2}{A_1}\frac{\delta_2}{\delta_1}\exp\psi\right)^{-1}\left(\frac{A_2}{A_1}\frac{1}{\delta_1}\frac{\partial \delta_2}{\partial V}\exp\psi - \frac{A_2}{A_1}\frac{\delta_2}{\delta_1^2}\frac{\partial \delta_1}{\partial V}\exp\psi + \frac{A_2}{A_1}\frac{\delta_2}{\delta_1}\theta_e^{-1}\exp\psi\right) \quad (12)$$

We differentiate Eqs. (1) and (10), and substitute these results, namely

$$\partial j_i^*/\partial V = (\partial j_{i,\infty}^*/\partial V)\gamma + j_{i,\infty}^*\partial\gamma/\partial V$$

$$\theta_e^{-1} = \partial\chi_{p1}/\partial V - \partial\chi_{p2}/\partial V$$

into Eq. (12), thereby eliminating the nonmeasurable $\psi \to 0$ value of the slope of the ion current from that expression. We then take the $\psi = 0$ limit of the resulting expression and rearrange terms, and the electron temperature measurement is found to be defined by

$$\theta_e = -\left[\frac{j_{i_1}^* j_{i_2}^*}{j_{i_1}^* + (A_2/A_1)j_{i_2}^*}\left(\frac{A_2}{A_1}\right)\frac{1}{(\partial h^*/\partial V)}(1+\sigma)\right]_{V=0} \quad (13)$$

where

$$\sigma|_{V=0} = \alpha\chi_f^{-1} - \gamma_f Z_f + \delta_f Y_f \quad (14)$$

$$Y = 1 - \delta^{-1} - \frac{1}{2}(1+K_e)^{-1}\alpha\left[\frac{\exp(-\chi_p)}{\chi_p}\frac{G_e(\tau)}{(j_{i,\infty}^*)^{1/2}} - \frac{2}{\chi_p}\right] + K_e^{-1}(1+K_e)^{-1}\exp(-\chi_p)\left[\left(\ln\frac{lx_0}{r}\right) + \frac{\chi_p}{\beta^{1/2}x_0\ln\{(x_0^2-1)^{1/2}+x_0\} + \chi_p/[2\ln(l/rx_0)]}\right]$$

$$Z = \alpha\chi_p^{-1}\tau^{1/2}(1+K_i)^{-1}\left\{\frac{1}{2}G_i(\tau)(j_{i,\infty}^*)^{1/2} + \alpha j_{i,\infty}^*[E_1(\tau\ln 2) - E_1(\tau\chi_p)] + (j_{i,\infty}^*)\exp(-\tau\chi_p)\right\} + K_i^{-1}(1+K_i)^{-1}\left(\frac{\tau^{1/2}}{1+\tau}\right)j_{i,\infty}^*\left\{\alpha\chi_p^{-1}\ln\frac{l}{rx_0} - \frac{1}{\beta^{1/2}x_0\ln\{(x_0^2-1)^{1/2}+x_0\} + \chi_p/2\ln(l/rx_0)}\right\}$$

All the relevant terms in the expressions of Eq. (14) are evaluated at $\chi_p = \chi_f$. Equation (13) is similar to the original Johnson and Malter[14] result except that the electron temperature θ_e is modified by a correction factor σ where

$$\sigma = \sigma(r/\lambda_d, K_{i,e}, l/r, \tau)$$

Values of σ have been calculated, using Eq. (14), for a wide range of r/λ_d and Knudsen number and are presented in Table 2. The correction factor is generally less than a few percent. This result is very encouraging because it means that the double probe may be used to measure electron temperatures in transition regions where the single probe characteristic cannot be interpreted.

Table 2 Temperature correction σ computed at T_e/T_i = 10 and l/r = 100 vs $K_e = K_i$ and r/λ_d

	r/λ_d				
K_e, K_i	80	40	10	4	2
100	0.017	0.026	0.057	0.089	0.105
10	0.014	0.021	0.047	0.074	0.086
3	0.006	0.011	0.029	0.047	0.056
1	−0.012	−0.009	0.001	0.010	0.018
0.3	−0.044	−0.042	−0.036	−0.030	−0.024
0.1	−0.072	−0.070	−0.064	−0.059	−0.052

Table 3 Dimensions of the cylindrical Langmuir probes

$2r$	l/r
0.001	384
0.005	65.2
0.010	39.6
0.010	32.6
0.025	3.0
0.025	11.0
0.025	83.2
0.040	4.30
0.060	3.66
0.070	2.32

The charged particle number density is usually computed from the magnitude of the ion-saturation current using the measured value of electron temperature. For the transition region, Eq. (1) may be expressed in the form

$$J_i/T_e^{1/2}\{2\pi rl(k/2\pi m_i)^{1/2}e\} = n_e j_{i,\infty}^*\gamma \quad (15)$$

where the left side consists of measurable quantities and the right side is a function of n_i, τ, ξ_e, and λ_i. If λ_i and T_i are determinable by some means not involving Langmuir probe measurements, then, $n_e = zn_i$ may be determined from Eq. (15). Because both $j_{i,\infty}^*$ and γ are functions of n_e through their dependence on ξ_e, a short iteration procedure is required to solve Eq. (15).

Of the various theoretical results presented for a single probe, Eqs. (1–4) which give the effect of collisions on the ion saturation current are probably the most accurate and useful. The approximations made in the estimation of the collisional effects on electron current in the retarding field regime [Eqs. (5) and (6)] are somewhat more questionable than those used for the ion current calculation, and therefore less reliance can be placed on the quantitative predictions for electron current collection. The result given by Eq. (8) for the floating potential in the presence of collisional effects may be the least accurate, since it involves the equating of the expressions for ion and electron currents at small probe potentials where these expressions are subject to the greatest uncertainty. With some effort, the accuracy of these expressions could be improved. However, even though some of the quantitative predictions may be in doubt, the qualitative trends exhibited by the results are expected to be correct.

As regards the double probe result given by Eqs. (13) and (14), considerable uncertainty in values of the various collisional corrections can be accepted without altering the final conclusion that the collisional correction factor σ is small, and therefore that double probes can be used for the determination of electron temperature even when substantial collisional effects are present.

3.0 Experiment

The experiments were performed in the Plasma section of the Berkeley Rarefied Gas Facility. Details of this low-density wind tunnel and its associated instrumentation have been reported in Refs. 15 and 16. The relevant dimensions of the cylindrical probes used in the study are given in Table 3. Detailed information on probe construction, cleaning, circuitry, operation, etc., can be found in Refs. 15–17.

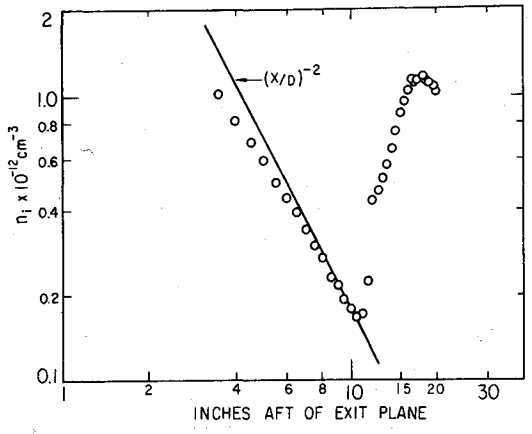

Fig. 6 Ion density measured along the centerline of freejet 1.

In order to investigate probe response over a wide range of the ratios of probe radius to Debye length and probe radius to relevant mean free path, experiments were performed in two partially-ionized argon freejet flows, referred to as Jet 1 and Jet 2. The properties of these flows were determined as described in Refs. 15–17, and are listed in Table 4.

All probe data reported here were obtained with cylindrical probes aligned with the flow direction. Since comparisons are made between these data and the theory described earlier, which pertains to a static plasma, a complete correspondence between the theory and the experiment is lacking, and the possible influence of convective effects must be considered. Two types of convective effects immediately come to mind, those associated with angle-of-attack caused by imperfect probe alignment, and those associated with collisional effects in the flowfield itself (i.e., the formation of shock waves and boundary layers on the probe). Both of these convective effects will be discussed in what follows.

4.0 Results

4.1 Ion Saturation Current Measurement

All ion saturation currents were measured at a probe potential $\chi_p = \chi_f - 10$, that is, ten dimensionless volts negative with respect to the floating potential. Using probes of varying size, measurements of ion saturation current and electron temperature were made along the centerlines of the two freejet flows. It was found that the ion number densities, inferred according to the theory of Laframboise, from the measurements made with the smaller probes were in self-agreement and followed the source-flow model of a freejet expansion, $n_i \sim (x/D)^{-2}$, as they should since it can be shown[16] that the ion concentration in these jet flows is "frozen." Data taken with the larger probes, when interpreted according to the theory of Laframboise, yielded apparent ion number densities which deviated from the source-flow prediction near the source, where the Knudsen numbers were in the transition range. The survey shown in Fig. 6, taken with a relatively large probe, shows the nature of the deviation.

The data obtained with the smallest probes were therefore used to establish the random ion current

$$J_r^* = 2\pi r l (kT_e/2\pi m_i)^{1/2} e n_e$$

along the jet centerlines, and using these data the dimensionless probe current

$$j_i^* = J_i/J_r^*$$

for all probes including those exhibiting transition effects could be established. All these probe data are plotted in Fig. 7, where they are compared with the theoretical prediction given by Eq. (1). Also shown are data obtained by Dunn and Lordi.[10] The theory is plotted for the nominal value of the aspect ratio parameter $l/r = 100$, although the data represent a range of this parameter. However, in the near-collisionless regime where most of the data fall j_i^* is a very weak function of l/r (the collisionless limit $j_{i,\infty}^*$ is independent of l/r), so that in the interest of presenting all the data on one plot a nominal value of the aspect ratio parameter was employed.

Table 4 Properties of freejet flows

	Freejet 1	Freejet 2
mass flow	1.41 g/sec	0.76 g/sec
stagnation temperature	1243°K	1940°K
stagnation pressure	9.3 torr	5.3 torr
static pressure[a]	0.090 torr	0.060 torr
static temperature[b]	53°K	74°K
$\lambda_{nn\infty}$*	0.2 cm	0.83 cm
M	3–9	3–8

[a] Static pressure in test chamber surrounding the freejet.
[b] In the freejet these values refer to the minimum density point ahead of the Mach disk.

It will be seen in Fig. 7 that both the present data and the data of Dunn and Lordi are in good agreement with the theory for $K_i \gtrsim 2$, whereas the data corresponding to the lowest Knudsen numbers are not, and in fact the agreement would have been poorer still had these data been compared with theory using the actual aspect ratios rather than the nominal one just mentioned.

There are several possible explanations for the poor agreement between experiment and theory for $K_i \lesssim 2$. One possibility is related to the fact that the theory employs for the continuum limit $j_{i,0}^*$ the large aspect ratio limit of the continuum current to an ellipsoidal probe, and therefore may be expected to be inaccurate for the small-aspect-ratio probes used to obtain the lowest Knudsen number data. The approximation for $j_{i,0}^*$ could have been improved, at some expense in complexity, by using the complete ellipsoidal probe theory, but this was not done.

The most likely reason for the poor agreement at the lowest Knudsen numbers is the presence of convective effects associated with shock wave formation ahead of the probe. Significant density increase in the flowfield in the neighborhood of a probe due to shock formation might be expected to occur for $K_i \lesssim 1$, and this could explain why the probes with the lowest Knudsen numbers yielded apparent ion number densities greater than the values predicted by the theory. Support for this conjecture is afforded by the fact that in the earlier comparison between the theory and the data of Kaegi and Chin reported in Ref. 8, good agreement between theory and experiment was obtained down to $K_i \approx 0.25$. The Kaegi-Chin data were obtained in the stagnation region of the shock layer on a blunt body, where convective effects would be expected to be smaller than those associated with the present experiment, and therefore the conditions of a static plasma required by the theory were more nearly realized. Thus, while the theory would appear to be useful for predicting transition effects on the ion current collected by aligned cylindrical probes in a flowing plasma only for $K_i \gtrsim 2$, it should be applicable at least to an order of magnitude lower Knudsen number in the case of a static plasma.

Our probes were found to be insensitive to small changes in angle of attack, and therefore possible slight misalignments were not critical. One cause for extreme sensitivity to small changes in angle of attack is the end effect reported by Hester and Sonin[18] which we show later in Sec. 4.3 to be negligible for our operating conditions. Small negatively-biased probes (i.e., those for which $r/\lambda_d < 1$) having an aspect ratio sufficiently large to eliminate this end effect were earlier found by Sonin[19] to also exhibit ion current collection which was quite sensitive to angle of attack variations. Hester and Sonin postulate that in this case sensitivity to angle of attack

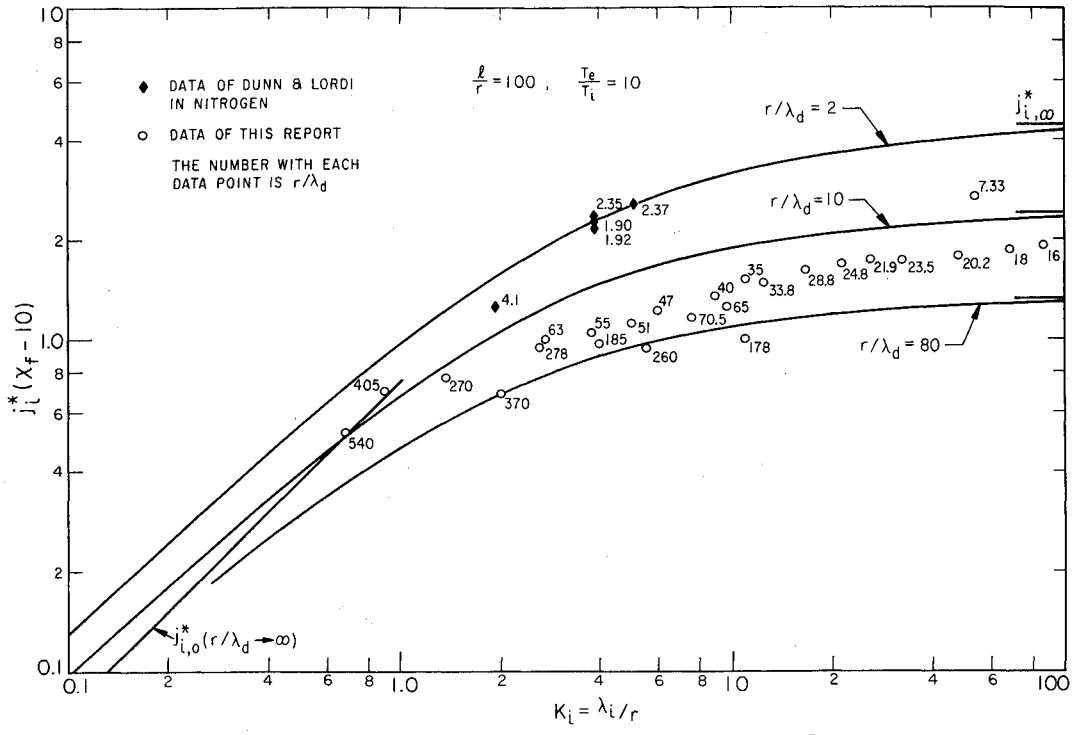

Fig. 7 Comparison between theoretical and measured probe current densities in the transition regime, taken at ten dimensional volts below the floating potential.

results because the ions are in "continuum flow" (the ion-ion free path was much smaller than the probe diameter) and move in essentially radial fashion toward the probe, if the probe is perfectly aligned with the flow. This is the condition for which the Allen-Boyd-Reynolds radial motion theory is presumed to apply. However, if the probe is at a slight angle of attack, Hester and Sonin argue that orbital motion instead of radial motion will result, and the ion current will be decreased from the radial motion limit toward the orbital motion of limit. The sensitivity to this type of angle-of-attack variation would be expected to lessen as r/λ_d is increased and in fact Sonin found that for $r/\lambda_d \approx 15$ an angle-of-attack change of 15° produced only about a 3% change in ion current collection. Although in the present experiment the ion-ion mean free path was as in Sonin's case much smaller than the probe diameter, r/λ_d exceeded 15 except for one data point, and therefore our observation of small angle-of-attack sensitivity is not inconsistent with the results of Sonin or of Hester and Sonin. Despite the fact that the ion-ion mean free path was smaller than the probe dimension in both the present work and in Sonin's experiment, the experimental evidence would appear to indicate that ion-ion self-collisions are unimportant as regards ion current collection by cylindrical probes in weakly ionized gases, provided that $r/\lambda_d \gtrsim 3$. However, a detailed analysis of the effect of such collisions has yet to be carried out.

4.2 Current Measurement in the Retarding Field Regime

Measurements of probe current in the range of probe potentials between the floating potential and the plasma potential, the so-called retarding-field regime, were carried out at various points along the axes of the freejets, using the probes listed in Table 3. These single-probe measurements were performed by displaying on the screen of a storage oscilloscope, as shown in Figs. 8–10, the logarithm of the probe current versus the probe potential resulting from about a 1 msec sweep of the probe potential, starting from the floating potential and ending somewhere beyond the plasma potential. Each photograph of the oscilloscope screen contains several successively obtained characteristics.

Three types of characteristic curves were observed, as shown in Figs. 8–10. Figure 8 shows a set of probe traces under a typical collisionless operating condition where the logarithm of the retarding-field current plotted vs the probe potential yields a straight line. Figure 9 shows results from a probe which yielded rounded characteristics near the plasma potential, and this condition will be termed the onset of transition. Figure 10 shows characteristic curves obtained from a probe operating in a fully transitional regime, and exhibiting inflection points in its characteristics.

It is difficult to ascribe the development of the inflection point in the retarding field characteristic to anything other than a collisional effect, since the data of Figs. 8–10 were obtained with three probes of progressively larger diameter located at the same point in the flow. An argument that the inflection points might be due to the existence of some form of non-Maxwellian electron energy distribution seems un-

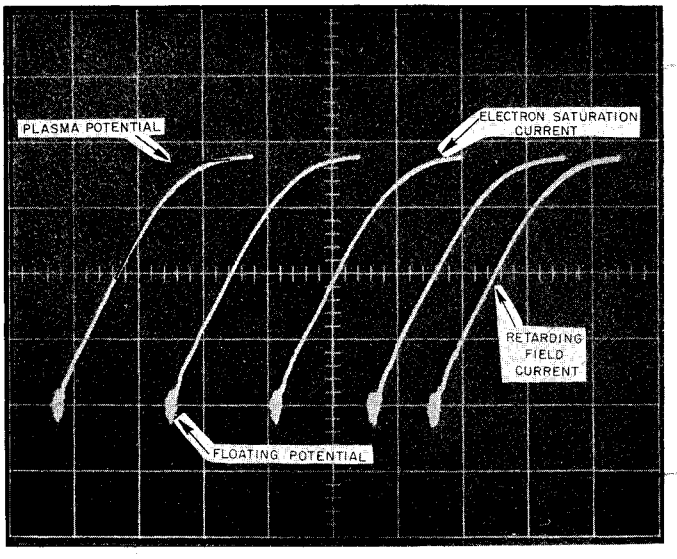

Fig. 8 Probe characteristics in the retarding-field regime, obtained under collisionless conditions.

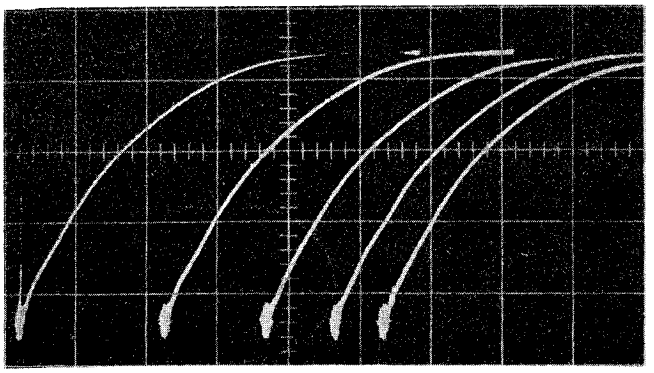

Fig. 9 Probe characteristics in the retarding-field regime, showing the onset of transitional effects.

tenable, since if this were the case the effect should have appeared on probes of all sizes at the point in question in the flow. Moreover, the absence of electric fields necessary sustain a non-Maxwellian electron distribution in the presence of a high electron self-collision frequency would make it difficult to argue the existence of such an energy distribution in any case.

A large number of probes were operated under the conditions represented by Figs. 8–10. The probe traces obtained were divided into the three classes indicated; those exhibiting essentially straight-line retarding-field characteristics, those exhibiting pronounced rounding of their characteristics in the vicinity of the plasma potential, and those exhibiting the behavior shown in Fig. 10. The results of the tests are shown in Fig. 11, on a plot of electron-ion probe Knudsen number vs λ_d/r. (The electron-ion mean free path was chosen for the correlation, rather than the electron-atom one, because the former was the smaller of the two, but the results would have been unchanged qualitatively if the latter mean free path had been used.) When the data were plotted in this way, it was found that the line $\lambda_{e-i} \cong 200\lambda_d$ separated the collisionless from the transitional data such that no transition effects are observed on the retarding field probe characteristic when $\lambda_{e-i} \gtrsim 200\lambda_d$. This manner of grouping the data is purely empirical, but it may possibly serve as a guideline as to when collisional effects will be observed on a cylindrical probe. It appears from Fig. 11 that, unlike the case of ion collection, the onset of transition effects in the retarding-field current is not correlated simply with a Knudsen number, but rather is a function of the Debye length-probe radius ratio as well.

Although the above remarks would suggest that the transition effects observed in the retarding field current are more complex than what is embraced in the theory, an attempt was made to compare an experimental fully-transitional retarding-field characteristic with the theory. The comparison, for a 0.01-in.-diam probe, is shown in Fig. 12. On the voltage scale the curves go from the floating potential to the plasma

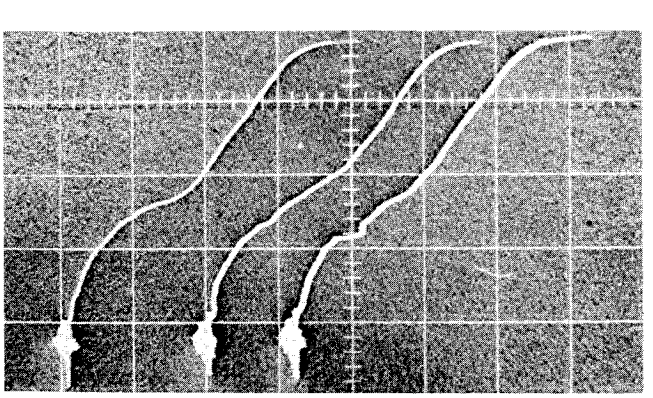

Fig. 10 Probe characteristics in the retarding-field regime exhibiting marked transitional effects.

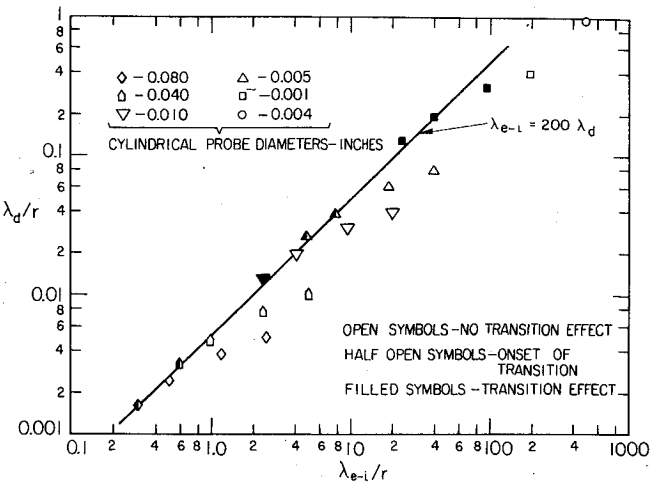

Fig. 11 Empirical correlation of λ_d/r vs λ_{e-i}/r for the onset of transition in the retarding-field probe characteristic.

potential, the latter being determined in the usual fashion by the intersection of the two straight lines which were judged to be the best fits to the linear parts of the retarding-field and the electron-saturation portions of the characteristics. The current scale is relative, i.e., $[j_e(m_i/m_e)^{1/2} - j_i^*]$ is normalized to unity at the plasma potential for the purpose of comparing the shapes of the theoretical and experimental characteristics.

The experimentally observed value of the floating potential for the case shown in Fig. 12 was $\chi_f = 11.9$, which is considerably greater than the nominal collisionless value of $\chi_f = 5.4$. An increase in floating potential due to collisional effects is predicted by the theory, but for the experimental conditions the theoretical increase, to $\chi_f = 6.16$, is much smaller than the experimental increase, and the theoretical curve does not have the inflection point exhibited by the experimental one. The inflection point and the large increase in χ_f do appear in the theory but at Knudsen numbers considerably smaller than those of the experiment, as can be seen from the theoretical curve constructed for $K_i = 10^{-3}$, $K_e = 10^{-2}$. All of the foregoing would seem to indicate that at best the theory gives only some qualitative indications of the effects of collisions

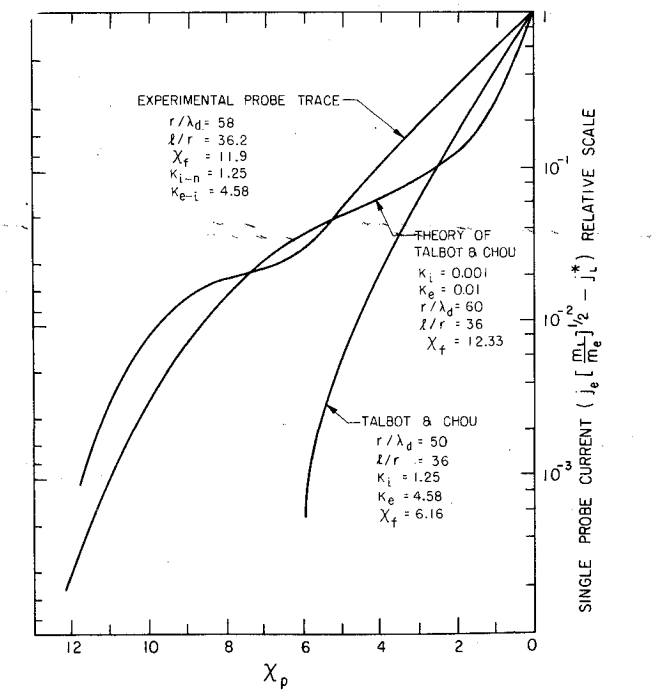

Fig. 12 Comparison between theoretical and experimental retarding-field characteristics.

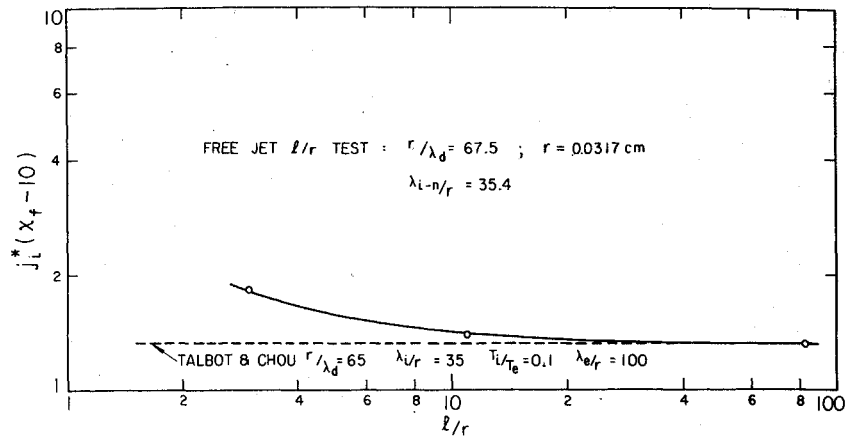

Fig. 13 Aspect ratio test results.

on the retarding-field characteristics of single probes and cannot be used for quantitative predictions. There is also the indication that contrary to the assumptions of the theory, the value of the parameter λ_d/r plays a role in determining the onset of transitional effects in the retarding field characteristic.

4.3 Aspect Ratio Measurements

Some experiments concerning the effect of probe aspect ratio l/r on the ion saturation current were also performed. Three probes of different aspect ratio but of the same radius were operated at one point in freejet 2. The point chosen for the tests was the minimum density point at the end of the source flow expansion just preceding the Mach disk. At this point in the jet the charged-particle number density was approximately constant over the length of the probe. The effect of a small aspect ratio on the ion current j_i^* to a probe in the near free molecule regime is shown in Fig. 13. A number of phenomena could produce an increased current density at the small aspect ratios. These include incomplete electrical insulation of the probe tip, a local density increase resulting from end collisions, the "end effect" depending on the parameter $(l/\lambda_d)(kT_e/m_iU)$ discussed by Hester and Sonin,[18] or a transition from the cylindrical collisionless sheath behavior assumed in the theory to something approaching a "sphere-like" sheath behavior, which should depend on the parameter l/λ_d. Since the problem depends on the parameters, l/λ_d, r/λ_d, $\{(l/\lambda_d)[(kT_e/m_i)/U]\}$ and K, Fig. 13 is essentially a "single" data point and gives little indication of the response of these same probes under different flow conditions or of probes of different l/λ_d, r/λ_d, etc., in these same flow conditions. Obviously, because of the number of parameters involved, an extensive parametric study would be required in order to determine the small aspect ratio effects for the various probes and flow conditions.

All data presented in this study were obtained with probes having $l/\lambda_d \gtrsim 500$, and $\{(l/\lambda_d)[(kT_e/m_i)/U]\} \gg 1$, including those having the smallest aspect ratios. Under these conditions both the "end effect" of Hester and Sonin and "sphere-like" sheath effect should be small. Since the effects of incomplete tip insulation and end collisions become negligible as the probe diameter becomes small (l/r becomes large) the data obtained in this report and presented in Fig. 7 should represent (except possibly for the very large probes) solely the influence of collisions on the probe response, as is implied in comparing the data with the Talbot-Chou theory. A more complete study of the aspect-ratio effect would be of use.

4.4 Electron Temperature Measurements with Double Probes

A number of double probe characteristics were obtained at various x/D locations in the jets in order to examine the effects of collisions on the determination of electron temperature. Figure 14 shows two typical characteristics, one obtained at a Knudsen number $K_{i-n} = 58$, and the other at a Knudsen number $K_{i-n} = 0.44$. (The current and voltage scales for Fig. 14 were made arbitrary for the purpose of comparing the two characteristics.) Although the characteristics in the collisionless and transition regimes are quite different, it was found that when they were used to obtain the electron temperature according to the method described in Ref. 20, both types of characteristics yielded the same electron temperature, $\theta_e = 0.15$ ev, within the usual experimental uncertainty. Comparisons of this nature thus provided experimental confirmation of the theoretical prediction cited earlier that the effect of collisions on electron temperature measurement with double probes is small.

The results also suggest that the cylindrical double probe configuration when used to determine electron temperature, may be less sensitive to convective effects than is the single probe, since the electron temperature measurements obtained with various double probes were in agreement even at Knudsen numbers less than unity, whereas the single probe ion current measurements at the lowest Knudsen numbers probably were influenced by convection. The reason for the apparent lack of sensitivity to convective effects of the double probes is not clear; it may simply be due to a fortuitous cancellation of the effects.

5.0 Conclusions

The theory of Talbot and Chou describing the effects of collisions on ion current collection of cylindrical Langmuir probes aligned with the flow direction appears to be useful for correcting ion current measurements made in the near-free-molecule flow regime. Departures between theory and experiment observed when the measurements were carried farther into the transition regime are probably due to the onset

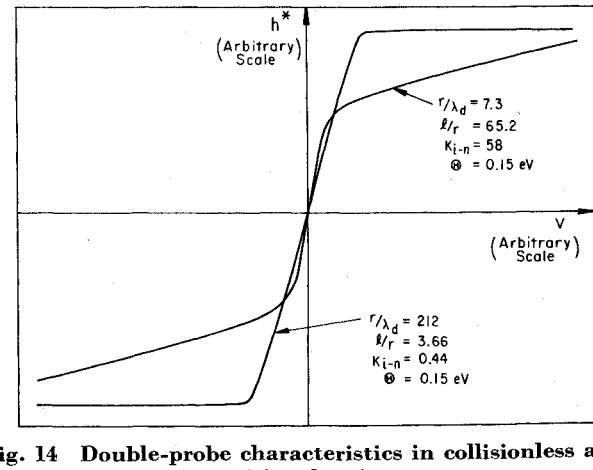

Fig. 14 Double-probe characteristics in collisionless and transitional regimes.

of convective effects, which are not accounted for in the theory, and thus possibly the theory may have a wider range of validity than is indicated by the present experiments, in the case of cylindrical probes operated in static plasmas. The predictions of the theory regarding the effects of collisions on current collection of single cylindrical probes in the retarding-field regime agree qualitatively but not quantitatively with the experiments. However, the prediction that the effect of collisions on electron temperature determination by means of double probes is small was confirmed by the experiments.

References

[1] Schultz, G. J. and Brown, S. C., "Microwave Study of Positive Ion Collection by Probes," *Physical Review*, Vol. 98, No. 6, June 15, 1955, pp. 1642–1649.

[2] Waymouth, J. F., "Perturbation of a Plasma by a Probe," *The Physics of Fluids*, Vol. 7, No. 11, Nov. 1964, pp. 1843–1854.

[3] Ecker, G., Masterson, K. S., and McClure, J. J., "Probe Theory in a Dense Plasma," UCRL-1028, TID-4500 (17th ed.), March 21, 1962, Radiation Lab., Univ. of California, Berkeley.

[4] Zakharova, V. M., Kagan, Y. M., Mustafin, K. S., and Perel, V. I., "Probe Measurements at Medium Pressures," *Zhurnal Teckhnicheskoi Fisiki*, Vol. 30, No. 4, April 1960, pp. 442–449.

[5] Wasserstrom, E., Su, C. H., and Probstein, R. F., "Kinetic Theory Approach to Electrostatic Probes," *The Physics of Fluids*, Vol. 8, No. 1, Jan. 1965, pp. 56–72.

[6] Chou, Y. S., Talbot, L., and Willis, D. R., "Kinetic Theory of a Spherical Electrostatic Probe in a Stationary Plasma," *The Physics of Fluids*, Vol. 9, No. 11, Nov. 1966, pp. 2150–2167.

[7] Bienkowski, G. K. and Chang, K. W., "Asymptotic Theory of a Spherical Electrostatic Probe in a Stationary Weakly Ionized Plasma," *The Physics of Fluids*, Vol. 11, No. 4, April 1968, pp. 784–799.

[8] Kaegi, E. M. and Chin, R., "Stagnation Region Shock Layer Ionization Measurements in Hypersonic Air Flows," AIAA Paper 66-167, Monterey, Calif., 1966.

[9] Talbot, L. and Chou, Y. S., "Langmuir Probe Response in the Transition Regime," *Rarefied Gas Dynamics*, Vol. 2, edited by C. L. Brundin, Academic Press, New York, 1969, pp. 1723–1737.

[10] Dunn, M. G. and Lordi, J. A., "Thin Wire Langmuir Probe Measurements in the Transition and Free Molecule Regimes," *AIAA Journal*, Vol. 7, No. 8, Aug. 1969, pp. 1458–1464.

[11] Laframboise, J. G., "Theory of Spherical and Cylindrical Langmuir Probes in a Collisionless, Maxwellian Plasma at Rest," No. 100, 1966, Univ. of Toronto Institute for Aerospace Studies.

[12] Abramowitz, M. and Stegun, I. A., *Handbook of Mathematical Functions*, Dover, New York, 1965, pp. 227–251.

[13] Cohen, J. M., "Asymptotic Theory of Ellipsoidal Electrostatic Probes in a Slightly Ionized, Callision-Dominated Gas," *AIAA Journal*, Vol. 5, No. 1, Jan. 1967, pp. 63–69.

[14] Johnson, E. O. and Malter, L., "A Floating Double-Probe Method for Measurements in Gas Discharges," *Physical Review*, Vol. 80, No. 1, Oct. 1, 1950, pp. 58–68.

[15] Peterson, E. W. and Talbot, L., "Langmuir Probe Response in a Turbulent Plasma," *AIAA Journal*, Vol. 8, No. 8, Aug. 1970, pp. 1391–1398.

[16] Kirchhoff, R. H. and Talbot, L., "An Experimental Study of the Shock Structure in a Partially Ionized Gas," *AIAA Journal*, Vol. 9, No. 6, June 1971, pp. 1098–1104.

[17] Kirchhoff, R. H., Peterson, E. W., and Talbot, L., "An Experimental Study of the Cylindrical Langmuir Probe Response in the Transition Regime," AS-69-13, Dec. 1969, Aeronautical Sciences Div., Univ. of California, Berkeley.

[18] Hester, S. D. and Sonin, A. A., "Ion Temperature Sensitive End Effect in Cylindrical Langmuir Probe Response at Ionospheric Satellite Conditions," *The Physics of Fluids*, Vol. 13, No. 5, May 1970, pp. 1265–1274.

[19] Sonin, A. A., "Free-Molecule Langmuir Probe and Its Use in Flowfield Studies," *AIAA Journal*, Vol. 4, No. 3, Sept. 1966, pp. 1588–1596.

[20] Peterson, E. W. and Talbot, L., "Collisionless Electrostatic Single-Probe and Double-Probe Measurements," *AIAA Journal*, Vol. 8, No. 12, Dec. 1970, pp. 2215–2219.